

HST/STIS spectroscopy of the magnetic Of?p star HD108: the low state at ultraviolet wavelengths

W. L. F. Marcolino^{1*}, J.-C. Bouret^{2,3}, N. R. Walborn⁴, I. D. Howarth⁵, Y. Nazé⁶, A. W. Fullerton⁴, G. A. Wade⁷, D. J. Hillier⁸ and A. Herrero^{9,10}

¹Observatório do Valongo, Universidade Federal do Rio de Janeiro, Ladeira Pedro Antônio, 43, CEP 20080-090, Brasil

²LAM-UMR6110, CNRS & Université Provence, rue Frédéric Joliot-Curie, F-13388 Marseille Cedex 13, France

³NASA/GSFC, Code 665, Greenbelt, MD 20771, USA

⁴Space Telescope Science Institute, 3700 San Martin Drive, Baltimore, MD 21218, USA

⁵Department of Physics and Astronomy, University College London, Gower Street, London, WC1E 6BT, UK

⁶FNRS-GAPHE, Département AGO, Université de Liège, Allée du 6 Août 17, Bat. B5C, B400-Liège, Belgium

⁷Department of Physics, Royal Military College of Canada, PO Box 17000, Station Forces, Kingston, ON K7K 7B4, Canada

⁸Department of Physics and Astronomy, University of Pittsburgh, Pittsburgh, PA 15260

⁹Instituto de Astrofísica de Canarias, C/ Vía Láctea s/n, E-38200 La Laguna, Tenerife, Spain

¹⁰Departamento de Astrofísica, Universidad de La Laguna, Avda. Astrofísico Francisco Sánchez s/n, E-38071 La Laguna, Tenerife, Spain

Received; Accepted

ABSTRACT

We present the first ultraviolet spectrum of the peculiar, magnetic Of?p star HD 108 obtained in its spectroscopic low state. The new data, obtained with the Space Telescope Imaging Spectrograph (*STIS*) on the *Hubble Space Telescope*, reveal significant changes compared to *IUE* spectra obtained in the high state: N v λ 1240, Si iv λ 1400, and C iv λ 1550 present weaker P-Cygni profiles (less absorption) in the new data, while N iv λ 1718 absorption is deeper, without the clear wind signature evident in the high state. Such changes contrast with those found in other magnetic massive stars, where *more* absorption is observed in the resonance doublets when the sightline is close to the plane of the magnetic equator. The new data show also that the photospheric Fe iv forest, at \sim 1600–1700Å, has strengthened compared to previous observations. The ultraviolet variability is large compared to that found in typical, non-magnetic O stars, but moderate when compared to the high-/low-state changes reported in the optical spectrum of HD 108 over several decades. We use non-LTE expanding-atmosphere models to analyze the new *STIS* observations. Overall, the results are in accord with a scenario in which the optical variability is mainly produced by magnetically constrained gas, close to the photosphere. The relatively modest changes found in the main ultraviolet wind lines suggest that the stellar wind is not substantially variable on a global scale. Nonetheless, multidimensional radiative-transfer models may be needed to understand some of the phenomena observed.

Key words: stars: winds – stars: atmospheres – stars: massive – stars: magnetic fields.

1 INTRODUCTION

The Of?p spectroscopic classification was introduced to describe a small group of O-type stars showing emission in the C III lines at 4650 Å at a strength comparable to that of the N III lines at 4634–42 Å (Walborn 1972). Normally, C III is weaker, or absent, in Of-star spectra. To date, only five stars belonging to the Of?p class have been found in

the Galaxy: HD 108, HD 148937, HD 191612, NGC 1624-2, and CPD–28° 2561, with the last two identified only recently (Walborn et al. 2010).

Substantial spectroscopic variability is now known to be an inherent property of the Of?p stars, with hydrogen and helium lines in the optical observed to vary between emission and absorption states on timescales that range from days to decades in different objects (Nazé et al. 2001; Walborn et al. 2003); the C III λ 4650 emission varies in concert with the hydrogen lines. The spectroscopic changes appear

* E-Mail: wagner@astro.ufrj.br

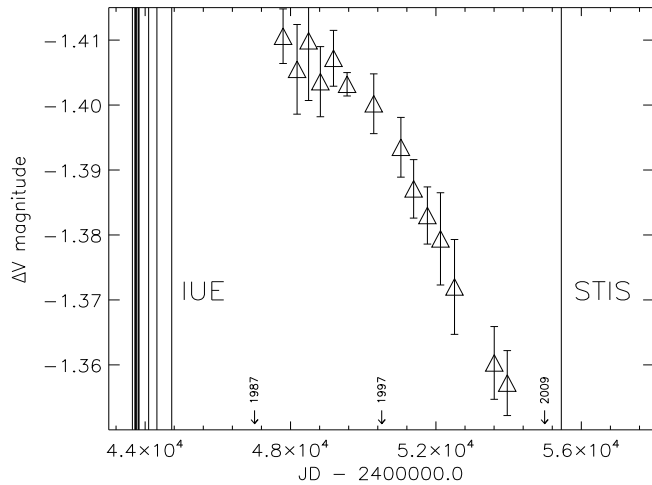


Figure 1. V-magnitude light-curve of HD 108 as a function of the Julian Day (data from Barannikov 2007). The observation dates of the *IUE* (made before 1982) and *STIS* (2010) data are indicated by vertical lines; photometric maximum corresponds to the spectroscopic high state (*IUE* observations), and vice versa. Arrows indicate observation dates of spectra displayed in Fig. 2.

to correlate with low-level photometric variability, such that the stars are a few per cent brighter in the optical when $H\alpha$ has maximum emission (e.g., Howarth et al. 2007; Barannikov 2007). Throughout this paper, the optical-spectrum emission and absorption states will be referred to as ‘high’ and ‘low’ states.

A crucial step towards an understanding of the Of?p phenomenon was made recently, with the detection of surface magnetic fields in HD 191612, HD 148937, and HD 108 (Donati et al. 2002; Wade et al. 2011; Hubrig et al. 2008, 2011; Martins et al. 2010 - hereinafter Paper I). The spectral variability is associated with magnetically constrained gas, whose aspect is rotationally modulated. The presence of a magnetic field could also potentially explain the exceptional X-ray luminosities of Of?p stars, observed to be above the O-star average (Nazé et al. 2010).

Ultraviolet (UV) spectra of massive stars are of particular interest, not least because they present the most sensitive diagnostics of stellar winds; but while the optical spectra of Of?p stars have been studied in detail for several years (e.g., Nazé et al. 2001, 2010), characteristics of their ultraviolet spectra are poorly known. For example, it is unclear to what extent the UV is variable (if at all), despite some efforts based on the sparse available data (e.g., Howarth et al. 2007). Are line-profile changes as intense as those observed in the optical? What are the consequences in terms of stellar physical properties?

Until now, we have lacked UV spectra for Of?p stars taken at contrasting optical states but with consistent wavelength intervals and comparable resolutions. Consequently, it is not yet known whether their wind properties are subject to change (either globally, or simply as a viewing effect), or to what extent the magnetic field influences the stellar atmosphere as a whole. In this context, new observational data are crucial for a better understanding of the Of?p class and the effects of magnetic wind confinement. They can also

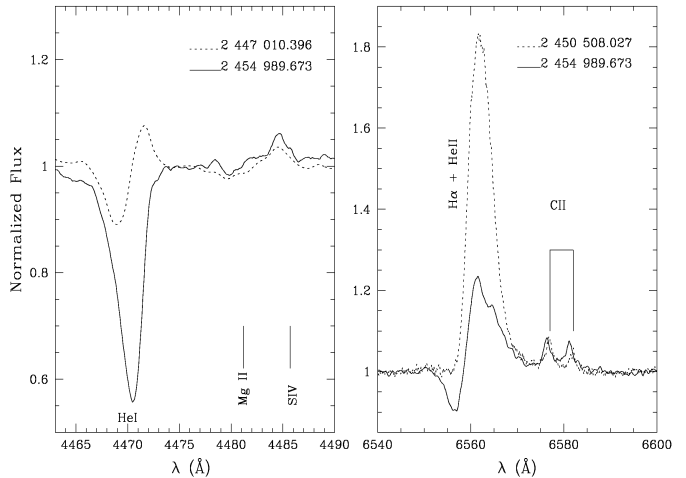


Figure 2. The low state of HD 108 (solid line; data from 2009) and two higher states (dotted-lines; data from 1987 and 1997). Exact Julian Dates are indicated. Note the drastic profile changes of $He\ I\ \lambda 4471$ and $H\alpha$. These states correlate well with photometric data (see arrows in Fig. 1).

provide empirical information to be compared to predictions provided by MHD simulations (e.g., ud-Doula et al. 2009)

In the present paper, we report the first high-resolution ultraviolet spectra of the Of?p star HD 108 in its low state. HD 108 is hot (~ 35 kK), massive ($\sim 40 M_{\odot}$), and harbours a relatively intense magnetic field (1–2 kG; Paper I). This field is considered to be responsible for the observed optical variability, modulated on a rotational period of about 55 years. Since HD 108 can be considered a prototype of the Of?p class (Walborn 1972), we expect the results and conclusions drawn from the present work to be applicable to other Of?p stars.

The paper is structured as follows: in Section 2 we present and describe the new UV data, acquired with the Hubble Space Telescope (*HST*). We compare them with archival spectra from the International Ultraviolet Explorer (*IUE*) satellite, obtained when HD 108 was in its optical high state. The main differences are discussed. Section 3 presents expanding-atmosphere (CMFGEN) models used to analyze the observations. Possible changes in the physical parameters with respect to previous analyses are discussed. The main results and conclusions are summarized in Section 4, where the significance of ultraviolet variability of HD 108, and the consequences for the interpretation of the Of?p phenomenon, are reviewed.

2 ULTRAVIOLET SPECTROSCOPY

We used the Space Telescope Imaging Spectrograph (*STIS*) on board *HST* to obtain ultraviolet spectra of HD 108 in 2010 September (P.I. Bouret). The observations were made using the FUV-MAMA and NUV-MAMA detectors, with the E140M and E230M echelle gratings. The wavelength coverage is ~ 1150 – 1750 Å (E140M) and 2250 – 3150 Å (E230M), with resolving powers of $R = 45,800$ and $30,000$, respectively. The signal-to-noise ratio (SNR) of the data is ~ 30 . By reference to results reported by Nazé et al. (2010)

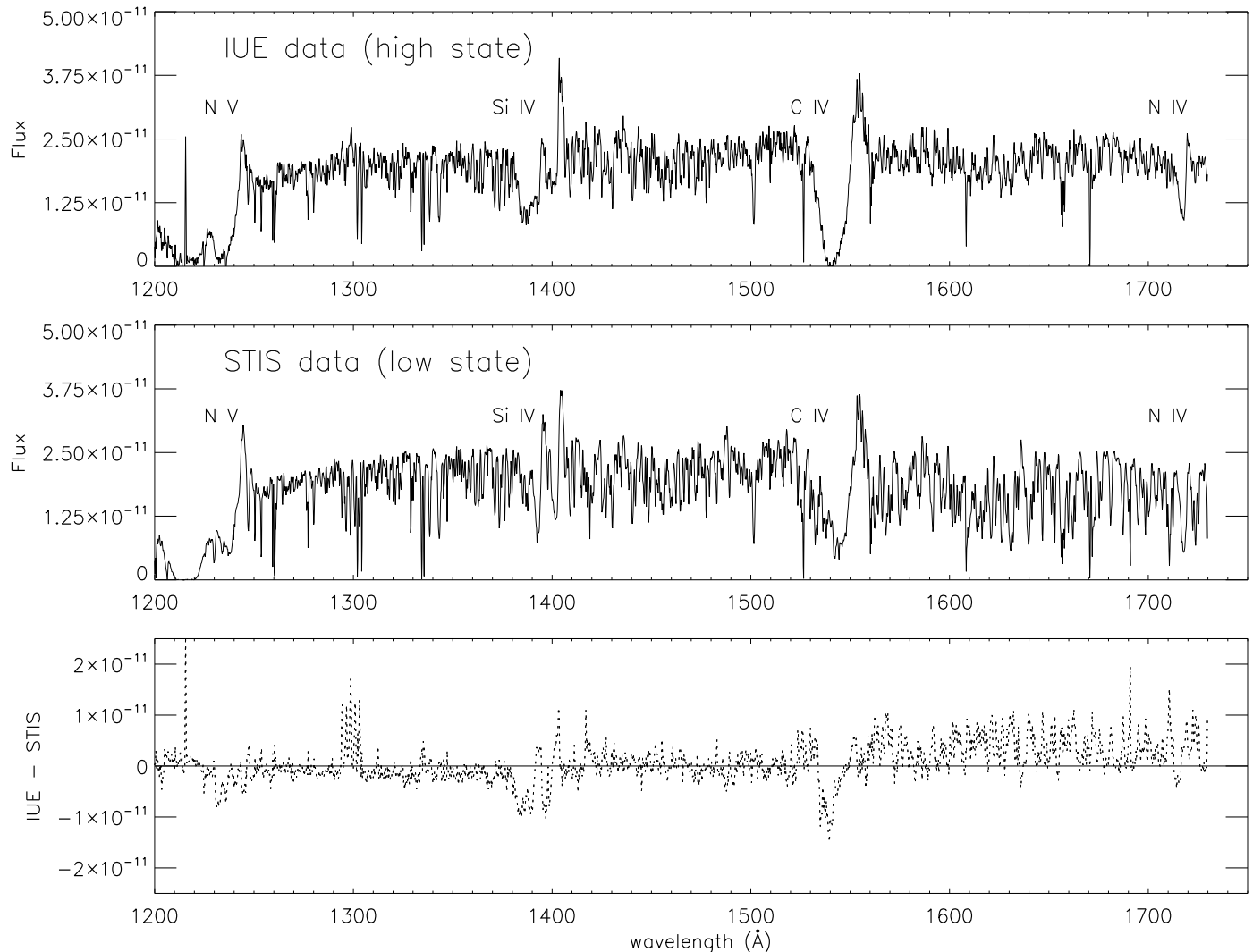


Figure 3. Ultraviolet spectra of HD 108 in the 1200–1750 Å range. Upper panel: *IUE* data acquired at the high state (SWP08352). Middle panel: new *STIS* data in the low state. Bottom panel: difference spectrum. Flux units are $\text{erg cm}^{-2} \text{s}^{-1} \text{Å}^{-1}$.

and photometry illustrated in Fig. 1, we infer that the observations were taken during the lowest emission-line state reached by HD 108, when it is faint in the BVR bands (Barannikov 2007) and the optical hydrogen and helium lines are in absorption, or have minimum emission compared to the high state. As an example, Fig. 2 presents optical profiles of He I $\lambda 4471$ and H α observed recently (in 2009) and decades ago (in 1997 and 1987).

Figure 3 presents the flux-calibrated *STIS* data for 1200–1750 Å, where the main wind lines occur. For comparison, we also plot *IUE* data (SWP08352) obtained when HD 108 was at its optical high state. Other *IUE* SWP observations show essentially the same spectrum, since they were also taken in the high state (Fig. 1). The resolving power and SNR of the *IUE* data ($R \simeq 10^4$ and ~ 10 , respectively) are poorer than for *STIS*, so both datasets were convolved to an effective resolution of 0.2 Å (FWHM).

2.1 Variability

Two general conclusions can immediately be drawn from Fig. 3. First, we do not observe *drastic* changes in the UV spectrum of HD 108 – that is, not as drastic as those observed in the optical spectrum, where intense high-state emission lines have turned into absorption lines over recent decades (Fig. 2; see also Nazé et al. 2001; 2010). The continuum level remains constant to within the combined observational uncertainties ($\sim 5\%$), so that the Of?p phenomenon does not cause the energy flux distribution in the UV to vary substantially. Moreover, the same basic set of photospheric and wind lines is present in both states, although with somewhat different profiles (see below). Qualitatively, it therefore seems that the global structure of the stellar wind is not severely modified by the magnetic field and that, with appropriate caveats, we may reasonably attempt to model the data with spherically symmetric models in the first instance.

On the other hand, it is clear that the observed variability very considerably exceeds that found in the UV spectra

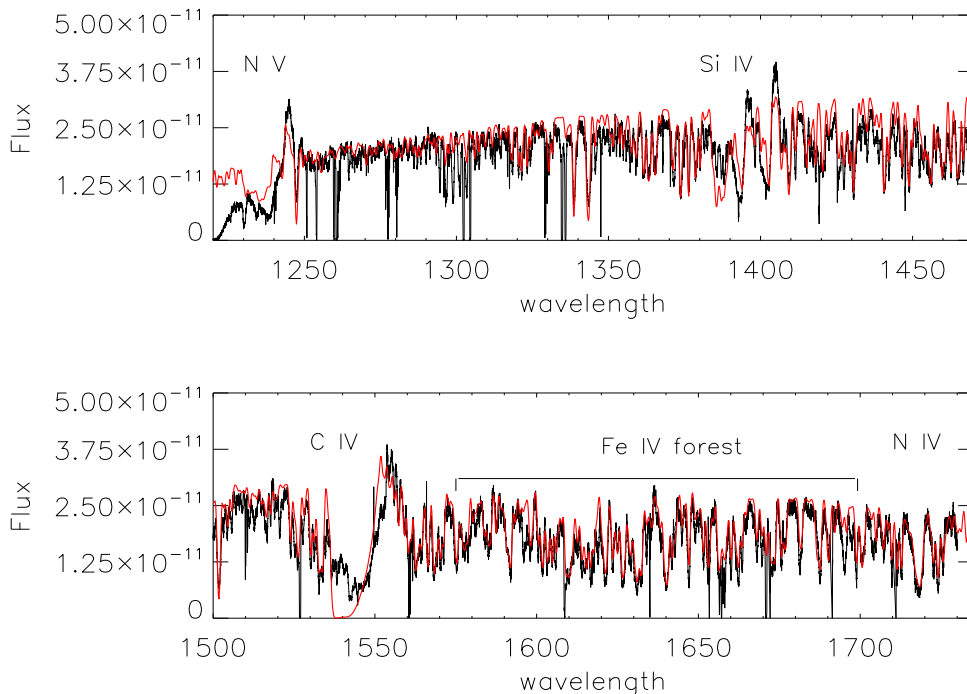


Figure 4. *STIS* low-state spectrum of HD 108 (black) compared with the adopted CMFGEN model (red). The stellar and wind parameters are as reported in Paper I, with the exception of the microturbulent velocity (Section 3.3; see Table 1). Note that, in this state, C IV $\lambda 1550$ is observed to have less absorption than predicted by the model (see text for more details). Flux units are $\text{erg cm}^{-2} \text{s}^{-1} \text{\AA}^{-1}$.

of *normal* O stars (cf., e.g., Kaper et al. 1996). There are clear changes between high- and low-state spectra in all the major wind lines: N V $\lambda 1240$, Si IV $\lambda 1400$, C IV $\lambda 1550$, and N IV $\lambda 1718$ (see the difference spectrum in Figure 3). In the low-state *STIS* spectrum, the subordinate N IV $\lambda 1718$ line has a deep/broad absorption profile without red wind emission, while the resonance lines exhibit P-Cygni profiles with reduced absorption. In particular, C IV $\lambda 1550$ now presents an unsaturated profile. The strengths of the P-Cygni emission components do not change, however, with the exception of N V $\lambda 1240$, which is somewhat stronger in the *STIS* spectrum than in the *IUE* data. As it is discussed later in the paper (see Section 4), a quantitative explanation for this fact, as well as for the decrease in the absorption of the resonance lines awaits more sophisticated MHD simulations. Nevertheless, we note that the different behavior of N V $\lambda 1240$ may be related to its higher sensitivity to X-rays (Hillier & Miller 2003; Marcolino et al. 2009). A small change in the number of X-rays photons available could potentially vary its emission level via Auger ionization. The photospheric iron forest also exhibits changes (especially beyond 1500\AA), being considerably stronger in the *STIS* data.

STIS data at wavelengths larger than 2250\AA (not shown) are comparatively featureless, with few, weak photospheric lines. An exception is C III $\lambda 2296$, which presents a relatively deep absorption. A detailed comparison with *IUE* spectra obtained at the high state is hindered by their resolution and, particularly, very poor SNR in this region.

2.2 Comparison with related systems

Interestingly, the changes in the P-Cygni profiles observed for HD 108 do not correlate with rotational phase in the same way as reported for magnetic B stars (see for example Shore et al. 1990; Henrichs et al. 2005). These stars normally present more absorption – e.g., in C IV – when the observer’s line of sight lies close to the plane of the magnetic equator. Such configuration corresponds to the low state of Of?p stars (see Wade et al. 2011b), i.e., the one analyzed in this paper.

The usual interpretation for magnetic B stars is that gas constrained by the magnetic field settles in a cooling disk about the magnetic equator; this disk would provide the extra absorption when observed edge-on (see however Section 4). We note however that such absorptions generally occur near the line center (i.e., low velocities), which points to corotating disk-like structures rather than a rapidly expanding wind.

The magnetic O dwarf star θ^1 Ori C follows the enhanced absorption scenario (Smith & Fullerton 2005). When its magnetic equator is edge-on ($\phi \simeq 0.5$) C IV $\lambda 1550$ shows enhanced blueshifted absorption relative to $\phi \simeq 0$. The red side of this feature also presents a small increase in flux at $\phi \simeq 0.5$; that is, the P-Cygni profile as a whole seems stronger when the magnetic equator is edge-on (see Fig. 3 in Smith & Fullerton 2005). At about this same phase, the H α profile has its minimum emission (Stahl et al. 1996). However, the situation in HD 108 is different: less absorption in C IV $\lambda 1550$ and minimum emission in H α are observed

when the line of sight lies close to the plane of the magnetic equator. This issue is discussed further in Section 4.

Besides HD 108 and θ^1 Ori C, four further O stars have detected magnetic fields: HD 191612, HD 148937, HD 57682, and ζ Ori A (Donati et al. 2006; Hubrig et al. 2008; Wade et al. 2011; Grunhut et al. 2009; Bouret et al. 2008). While all have estimated rotation periods, available UV data are insufficient to draw conclusions concerning wind-profile behaviour at specific phases. An exception is HD 191612. New UV observations of this star were recently acquired by our group and a detailed analysis will be presented in a forthcoming paper.

3 MODEL ATMOSPHERES

We have used CMFGEN (Hillier & Miller 1998) to generate non-LTE models to analyze the new *STIS* observations of HD 108. CMFGEN solves the equation of radiative transfer in a spherically symmetric outflow under the constraints of radiative and statistical equilibria. Further model assumptions, and basic procedures for the determination of parameters, are as described in detail in Paper I.

In Paper I we obtained a reasonable fit to optical (low state), UV (*IUE*; high state), and far-UV (*FUSE*; low state) data of HD 108 with a single model. Since the UV and far-UV observations were obtained in different states, it was tentatively concluded that the global stellar-wind properties may be stable in spite of the large changes occurring in the optical lines (and attributed to a localised, magnetically constrained plasma). In order to examine this idea, we began the spectral analysis with the set of parameters derived in Paper I. After several exploratory models, we concluded that, notwithstanding some discrepancies, these basic parameters also represent the new *STIS* data reasonably well. The problems and improvements found during our analysis are discussed below. Our adopted best-fit model is shown in Fig. 4 and the stellar and wind properties are summarized in Table 1.

3.1 Mass-loss rate

In order to desaturate the model C IV $\lambda 1550$ P-Cygni profile, to better match the *STIS* data (Fig. 3), we initially adjusted the mass-loss rate \dot{M} to decrease the stellar-wind density. A match could only be achieved by reducing the mass-loss rate by an order of magnitude (to $\sim 10^{-8} M_{\odot} \text{ yr}^{-1}$). However, while the observed intensities of C IV $\lambda 1550$ and N V $\lambda 1240$ are then correctly predicted, their full profiles are not reproduced in detail – the synthetic lines lack P-Cygni absorption at low velocities. Furthermore, the C III $\lambda 1176$ and Si IV $\lambda 1400$ lines are predicted to be purely photospheric, while *STIS* data reveal conspicuous P-Cygni profiles (see Section 3.3 for fits to C III $\lambda 1176$).

We could find no model that simultaneously reproduces, in detail, both C IV $\lambda 1550$ and the weaker P-Cygni profiles observed in the *STIS* spectrum (C III $\lambda 1176$, N V $\lambda 1240$, Si IV $\lambda 1400$). We explored other ways to decrease the intensity of the wind profiles (e.g., adjusting the wind clumping and the X-ray distribution and luminosity) but they all turned out to be unsuccessful. Nevertheless, given the problems that arose in adopting lower mass-loss rates, we con-

Table 1. Stellar and wind properties of HD108.

T_{eff} (K)	$35\,000 \pm 2000$
$\log g$ (cgs)	3.50 ± 0.20
$\log L_{\star}/L_{\odot}$	5.70 ± 0.10
R_{\star}/R_{\odot}	$19.2^{+3.3}_{-2.8}$
M_{\star}/M_{\odot}	43^{+32}_{-18}
$v_{eq} \sin i$ (km s $^{-1}$)	0
v_{mac} (km s $^{-1}$)	45
ξ_t^{phot} (km s $^{-1}$)	50
P_{rot} (yr)	50-60
$\log \dot{M}$	-7.0 ± 1.0
v_{∞} (km s $^{-1}$)	2000 ± 300
$\log L_X/L_{BOL}$	-6.2

sider the value of $\dot{M} = 10^{-7} M_{\odot} \text{ yr}^{-1}$ obtained in Paper I to be reasonable. However, in the light of the spectroscopic variability, we now adopt a more conservative uncertainty of ± 1 dex for this parameter. We return to this issue in Section 4.

3.2 Effective temperature and Fe abundance

The new *STIS* data show that the numerous Fe IV lines in the ~ 1600 – 1700 Å region – the iron forest – are stronger than in the high-state observations (Fig. 3). A possible cause for this variation is a change in the effective temperature, T_{eff} , which affects the balance between Fe III, Fe IV, and/or Fe V line intensities in the UV spectra of OB stars (the influence of other parameters is examined in the Section 3.3). We explored models with effective temperatures both higher and lower than the baseline value of 35 kK. The more intense iron forest in the *STIS* spectrum is best reproduced with a slightly reduced T_{eff} , in the range 32.5–34 kK. However, for the lower value of T_{eff} both C III $\lambda 1176$ and Si IV $\lambda 1400$ have very strong wind signatures in the models, in stark contrast with the observations.

Our conclusion is that the new *STIS* data are better matched with a slightly lower effective temperature than the value inferred in Paper I, which was based only on helium lines. However, the difference is comfortably within the previously adopted uncertainty of 2 kK.

Given the results reported above and in the previous section regarding the C III $\lambda 1176$ and Si IV $\lambda 1400$ lines, we also explored the effects of models in which effective temperatures below 35 kK were coupled with lower mass-loss rates. These models were unsuccessful in fitting all wind lines simultaneously; as the mass-loss rate decreases, the initially strong C III $\lambda 1176$ and Si IV $\lambda 1400$ features go into absorption long before C IV $\lambda 1550$ becomes desaturated.

Our models indicate that changes in the iron content also modify the strength of the Fe IV forest, as expected. An inhomogeneous distribution of iron in the photosphere, for example, could cause variability according to the stellar rotational period. However, we think this scenario is unlikely. It is hard to justify an increase in the abundance of this element much above the solar value (needed to fit the observations). Moreover, we recall that other lines are also stronger in the *STIS* data (compared to *IUE*), e.g., N IV $\lambda 1718$ and He II $\lambda 1640$. In the next section we discuss the parameter

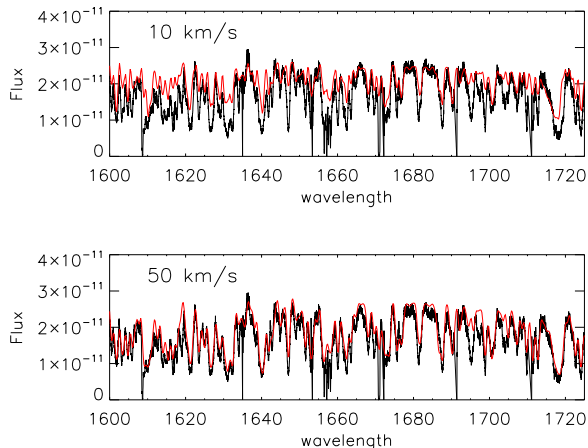


Figure 5. Effect of microturbulence on the modelled spectrum. Top panel: *STIS* spectrum (black) and model with $\xi_t^{\text{phot}} = 10 \text{ km s}^{-1}$ (red). Lower panel: *STIS* spectrum and model with $\xi_t^{\text{phot}} = 50 \text{ km s}^{-1}$. Better agreement is achieved using the higher ξ_t^{phot} for the Fe IV forest, He II $\lambda 1640$, and N IV $\lambda 1718$. Flux units are $\text{erg cm}^{-2} \text{ s}^{-1} \text{ \AA}^{-1}$.

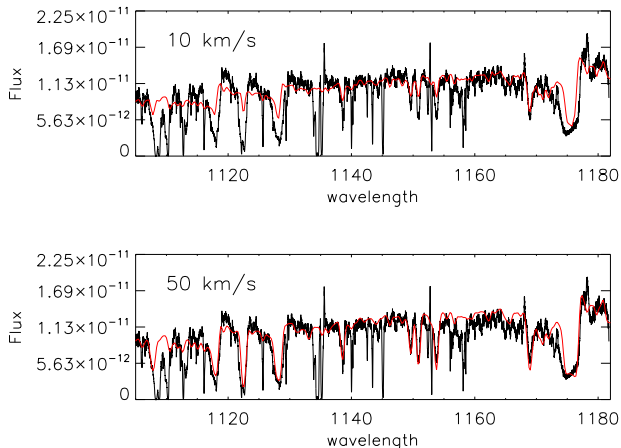


Figure 6. As Fig. 5 but for the *FUSE* spectrum. The deep, narrow absorption lines that are not predicted are of interstellar origin. A better agreement to most lines is achieved with a large turbulent velocity.

that was able to improve the fits to all these transitions and also the *FUSE* region, simultaneously.

3.3 Rotation, macroturbulence, and microturbulence

Other parameters affect the line profiles in the Fe IV forest, including the projected equatorial rotation velocity, $v_{\text{eq}} \sin i$; the macroturbulence; and the microturbulence. The first and the second parameters do not alter the line equivalent widths, W_λ , but merely redistribute the flux. Here, following the analysis performed in Paper I, we adopt a $v_{\text{eq}} \sin i$ of zero (consistent with the inferred very long rotation period) and a gaussian macroturbulent velocity of $v_{\text{mac}} = 45 \text{ km s}^{-1}$. Lower values produce deeper synthetic Fe IV profiles, but they are much narrower than observed (since W_λ is conserved). We recall that the origin, and hence a proper description, of the macroturbulence is still a matter of debate (see Simón-Díaz et al. 2010 and references therein).

The intensity of the Fe IV forest is also affected by the microturbulence, ξ_t . In CMFGEN, the comoving frame calculations are performed using ξ_t^{phot} , while the spectrum in the observer’s frame is computed by using a radially dependent turbulence parametrized by

$$\xi_t(r) = \xi_t^{\text{phot}} + (\xi_t^{\text{max}} - \xi_t^{\text{phot}}) \frac{v(r)}{v_\infty},$$

where $v(r)$ and v_∞ are the velocity field and terminal speed, respectively, and ξ_t^{max} corresponds to the maximum turbulent velocity (assumed to be about 10% of the terminal speed). This prescription mimics classical microturbulence at the photospheric level and the velocity dispersion from shocks occurring in the stellar wind (see Hillier et al. 2003 for details).

By varying ξ_t^{phot} from an initial value of 10 km s^{-1} up to 50 km s^{-1} we found progressively better fits to the iron forest in the *STIS* spectrum. Surprisingly, we also found a substantial improvement in the fits of a number of other lines. For example, we achieved excellent agreement with the deep, broad N IV $\lambda 1718$ line, and could much better reproduce the far-UV *FUSE* spectrum, which was analyzed in Paper I but with conspicuous discrepancies in line width and depth. We recall that neither $v_{\text{eq}} \sin i$, nor different macroturbulent values, were able to improve the fit to all these transitions.

Figs. 5 and 6 illustrate the effects of changing ξ_t^{phot} . We note that *FUSE* and *STIS* data below 1200 \AA are virtually identical, both being acquired in the low state. Although values of $\xi_t^{\text{phot}} \simeq 50 \text{ km s}^{-1}$ appear unrealistic for typical O stars, our results hint that some unknown turbulence may be at work, particularly at the configuration corresponding to the low state (cooling disk/magnetic equator edge-on). Note that such high turbulent velocities also affect the optical spectrum. However, the best fit we could achieve for this spectral region presents difficulties due to the observed presence of core line emissions and abnormally deep absorption profiles (see Paper I), hampering a reliable ξ_t^{phot} determination.

3.4 Line-formation regions vs Alfvén radius

In order to gain more insight into the influence of the magnetic field on the atmosphere of HD 108 we examined the radial extents of line-formation regions in our final model (Fig. 4) and compared them to the location of the Alfvén radius, calculated from

$$\left(\frac{R_A(\theta)}{R_*} \right)^{2q-2} - \left(\frac{R_A(\theta)}{R_*} \right)^{2q-3} = \eta_* (4 - 3 \sin^2 \theta)$$

(ud-Doula & Owocki 2002). For simplicity, we assume a confinement parameter $\eta_* = 100$ (Paper I), $\theta = 90^\circ$ (line of sight in the plane of the magnetic equator), and $q = 3$ (dipole field), giving $R_A \simeq 3.45 R_*$.

As an example, Fig. 7 shows the formation regions of the N IV $\lambda 1718$, C IV $\lambda 1550$, Si IV $\lambda 1400$, H α , and H β lines. The location of the Alfvén radius is indicated. The C IV and Si IV features are formed in a very extended region, encompassing R_A . N IV $\lambda 1718$ is formed closer to the photosphere but at the same time it goes farther than the Balmer lines. This is compatible with the moderate changes observed in the UV (Figure 3); the magnetic field is expected to have

a relatively modest influence as we get closer to the Alfvén radius and beyond. In contrast, $H\alpha$ and $H\beta$ are formed well below R_A , where the influence of the magnetic field on the gas distribution is more significant (see ud-Doula & Owocki 2002).

Our models, while providing a reasonable fit in the UV, predict pure-absorption Balmer profiles at all times. However, observations reveal large variability of some optical lines. For example, $H\beta$ has a very intense emission at the high state and an absorption profile at minimum (Nazé et al. 2010; see also the behavior of $H\alpha$ in Fig. 2). Fig. 7 thus suggests that the optical variability/emission observed is probably related to material constrained by the magnetic field close to the photosphere, below R_A . Currently, this constrained material is not modelled by CMFGEN or any other detailed atmosphere model.

4 DISCUSSION AND CONCLUSIONS

The intense optical variability presented by Of?p stars has been described in detail over the last decade. However, until now it has been unclear if variability would also be present at ultraviolet wavelengths. Consequently, it has been a matter of speculation as to whether the global stellar wind parameters of Of?p stars change through the different optical states observed.

A first qualitative result in this sense was reported by Howarth et al. (2007), for the Of?p star HD 191612. They reported that two UV spectra (from *IUE*) obtained in epochs of different optical spectra showed no large differences, suggesting that the global wind properties of HD 191612 (e.g., mass-loss rate) are not significantly modulated by the Of?p phenomenon. However, the comparison made by those authors was limited by having to use spectra at very different spectral resolutions, requiring degradation of the higher-resolution observation ($\sim 0.2\text{\AA}$) to match the lower-resolution data ($\sim 6\text{\AA}$). As a consequence, moderate variability could not be ruled out. Despite this, the large optical line changes observed were attributed to magnetically constrained material, mainly close to the photosphere, since otherwise the UV wind profiles would similarly be highly variable.

The present paper casts light on these issues by presenting, for the first time, new high-resolution ultraviolet spectra of HD 108 in the low state (very close to minimum; Nazé et al. 2010), alongside high-state data of comparable quality. The main results from our analysis are:

- The UV spectrum of HD 108 does not present variability as dramatic as that seen in the optical, where previously intense emission lines have changed into absorption features (or weak emission) in recent decades (see Fig. 2; see also Nazé et al. 2010). On the other hand, we emphasize that the UV variability is very large compared to that usually found in typical, non-magnetic O stars (see for example Kaper et al. 1996).

- The new *STIS* data reveal moderate differences compared to previous *IUE* data acquired at the high state. The low-state spectrum has somewhat less intense P-Cygni profiles (e.g., in N IV $\lambda 1240$ and C IV $\lambda 1550$). The photospheric iron forest is stronger, and the N IV $\lambda 1718$

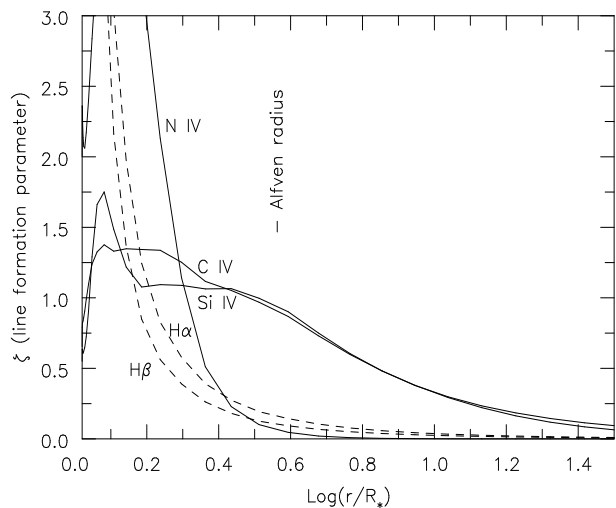


Figure 7. Line-formation regions of $H\alpha$, $H\beta$, N IV $\lambda 1718$, C IV $\lambda 1550$, and Si IV $\lambda 1400$. The Balmer and UV transitions are represented by dashed and solid lines, respectively. The location of the Alfvén radius (R_A) is indicated. Note that the Balmer lines are formed well below R_A , where the influence of the magnetic field is greatest.

line is deeper than in the high state, without an obvious wind profile. The UV continuum level remains constant, to within observational errors, between the low and high states.

- The analysis of the UV spectra through expanding-atmosphere CMFGEN models suggests that the wind properties of HD 108 at the optical low and high states remain essentially preserved, in agreement with the suggestion by Howarth et al. (2007) in the case of HD 191612. However, simultaneous fits to all UV wind lines proved elusive, suggesting that the mass-loss rate determination is somewhat uncertain. More sophisticated models may be needed to solve this issue.

Although moderate in scale compared to the optical, the variability revealed by the *HST* data carries important new information. The P-Cygni profiles of HD 108 vary in an opposite sense to those found in other magnetic OB stars. Usually, when the magnetic equator/cooling disk is seen edge-on, more absorption is detected in the UV resonance lines (e.g., θ^1 Ori C; Smith & Fullerton 2005). In HD 108, in this configuration, we detect *less* absorption in the wind profiles. This is illustrated for C IV $\lambda 1550$ and Si IV $\lambda 1400$ in Fig. 8.

At a first glance, more absorption is compatible with the density enhancements expected in the magnetic equatorial region due to gas confinement. However, this constrained material has also lower velocities compared to the flow at higher latitudes (e.g., ud-Doula et al. 2002). Therefore, the absorption should be less blueshifted and is expected to be less intense as a whole, as reported here for HD 108 (Sundqvist & ud-Doula; private comm.). In fact, MHD simulations for θ^1 Ori C fail to describe the observed C IV $\lambda 1550$ variability, predicting a less intense absorption profile when $\phi \sim 0.5$ (ud-Doula 2008).

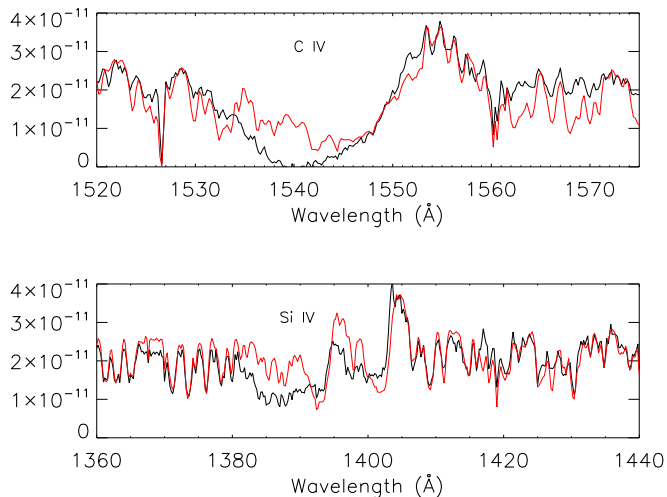


Figure 8. C IV $\lambda 1550$ and Si IV $\lambda 1400$ variability in HD 108. The profiles present more absorption at the high state (black line; *IUE* data) and are weaker at the low state (red line; magnetic equator edge-on; *STIS*). Other massive magnetic stars reveal the opposite when the magnetic equator/cooling disk is seen edge-on. Flux units are $\text{erg cm}^{-2} \text{s}^{-1} \text{\AA}^{-1}$.

An explanation for the contrasting behavior of the UV wind line variability in HD 108 and θ^1 Ori C (and other magnetic B stars) may reside in the nature of their cooling disks. Host stars with different physical parameters and magnetic field strengths could possess disks with different properties (e.g., ionization, density, and temperature). More or less absorption could be dictated by different ionization/recombination rates in each case. Indeed, HD 108 has a much higher mass ($\sim 40 M_{\odot}$) and luminosity ($\sim 5 \times 10^5 L_{\odot}$) than do B stars. Its luminosity, temperature, and radius are also considerably different from θ^1 Ori C (e.g., Donati et al. 2002). New MHD simulations coupled with radiative transfer calculations are needed to address such questions.

An alternative hypothesis for the UV variability in HD 108 which does not involve material accumulated in the magnetic equatorial region is simply a time-dependent stellar wind (stochastic variability). In this case, we would expect no correlation between rotational phase and the UV and optical line changes. Further monitoring would test this scenario.

For more constraints on these questions, it would be of interest to investigate whether the effect observed in Fig. 8 occurs in other Of?p stars. HD 191612 is particularly important, since its magnetic and rotational properties are relatively well studied (Howarth et al. 2007, Wade et al. 2011b). In this star, the $H\alpha$ equivalent-width and longitudinal-field measurements (B_z) are very reproducible on the 537.6-d rotation period (see Fig. 3 in Wade et al. 2011b). New *STIS* observations at different phases – including at magnetic equator edge-on ($\phi = 0.5$ and $|B_z| = 0$) – have recently been obtained by our group, and will elucidate the behavior of the P-Cygni profiles.

Another interesting issue raised by the new *HST* data is the strength of the iron forest compared to previous *IUE* (high-state) observations. Improved agreement with the Fe IV lines (and, surprisingly, with N IV $\lambda 1718$, He II $\lambda 1640$,

and other lines in the far UV) was achieved by adopting high turbulent velocities in the atmosphere models (up to 50 km s^{-1}). We speculate that shocks occurring about the magnetic equator would be a possible explanation for the origin of such high velocity dispersion in the inner regions (up to the Alfvén radius); this would be consistent with the less intense lines seen at other phases/viewing angles. This hypothesis should be examined in magnetic stars with physical properties similar to HD 108, and through MHD simulations.

Overall, the emerging scenario for Of?p stars is that their magnetic fields have a strong influence close to the photosphere, up to the Alfvén radius. Most of the observed spectral variability in the optical is expected to arise from this region – e.g., line profiles changing between intense emission and absorption states, and evidence for infall (see Paper I). The moderate UV wind-line variability (changes in W_{λ} much less than found in the optical) would reflect the fact that the extended stellar winds are less affected by the magnetic field on a global scale (see Fig. 7).

Notwithstanding that we have obtained a representative set of physical parameters that generate models matching the spectrum of HD 108 reasonably well, a precise determination of the stellar and wind parameters of Of?p stars awaits the construction of more sophisticated atmosphere and MHD models. As yet, we are unable to model/predict the spectrum of the gas which is strongly constrained by the magnetic field. The discrepancies highlighted in the analysis carried out here, and in our previous work (Paper I) suggest that our atmosphere models may be providing only rough estimates for the properties of these objects.

Although we do not expect a large degree of asphericity in the wind of HD 108 beyond the Alfvén radius – given the observed UV variability and the reasonable fit achieved with the current models (see Figures 3 and 4) – multidimensional radiative transfer models may be needed to explain the peculiar and variable optical and UV line profiles, in conformity with constrained material subjected to rotational modulation. As shown by MHD simulations, magnetically constrained winds may present a great diversity of effects (ud-Doula et al. 2002, 2006, 2009). Common assumptions, such as radiative equilibrium and a parametrized distribution of X-ray emission, may need to be revised as well.

ACKNOWLEDGMENTS

WLFM acknowledges support from the Fundação de Amparo à Pesquisa do Estado do Rio de Janeiro (FAPERJ/APQ1). NRW acknowledges support provided by NASA through grant GO-12179.01 from STScI, which is operated by AURA, Inc., under NASA contract NAS5-26555. YN acknowledges support from the Fonds National de la Recherche Scientifique (Belgium), the Communauté Française de Belgique, the PRODEX XMM and Integral contracts, and the 'Action de Recherche Concertée' (CFWB-Académie Wallonie Europe). GAW acknowledges Discovery Grant support from the Natural Sciences and Engineering Research Council of Canada (NSERC). AHD thanks support by the Spanish Ministerio de Ciencia e Innovación (grant AYA2010-21697-C05-04), the Consolider-Ingenio 2010 Program (CSD2006-00070) and the Gobierno

de Canarias (grant PID2010119). We thank the French Agence Nationale de la Recherche (ANR) for financial support. We also thank F. Martins, J. Sundqvist, and A. ud-Doula for valuable comments in an earlier version of the manuscript.

REFERENCES

- Barannikov, A. A., 2007, *Information Bulletin on Variable Stars*, 5756, 1
- Bouret, J.-C., Donati, J.-F., Martins F., Escolano C., Marcolino W., Lanz, T., Howarth, I. D., 2008, *MNRAS*, 389, 75
- Donati, J.-F., Babel, J., Harries, T. J., Howarth, I. D., Petit, P., Semel, M., 2002, *MNRAS*, 333, 55
- Donati, J.-F., Howarth, I. D., Bouret, J.-C., Petit, P., Catala, C., Landstreet, J., 2006, *MNRAS*, 365, L6
- Grunhut, J. H., Wade, G. A., Marcolino, W. L. F., et al., 2009, *MNRAS*, 400L, 94
- Henrichs, H. F., Schnerr, R. S., ten Kulve, E., 2005, *ASP Conference Series*, 337, 114
- Hillier, D. J., Miller, D. L., 1998, *ApJ*, 496, 407
- Hillier, D. J., Lanz, T., Heap, S. R., Hubeny, I., Smith, L., Evans, C. J., Lennon, D. J., Bouret, J.-C., 2003, *ApJ*, 588, 1039
- Howarth, I. D., Walborn, N. R., Lennon, D. J., Puls, J., Nazé, Y., Annuk, K., et al., 2007, *MNRAS*, 381, 433
- Hubrig, S., Scholler, M., Schnerr, R. S., González, J. F., Ignace, R., Henrichs, H. F., 2008, *A&A*, 490, 793
- Hubrig, S., Scholler, M., Kharchenko, N. V., Langer, N., de Wit, W. J., Ilyin, I., Kholtygin, A. F., Piskunov, A. E., Przybilla, N., 2011, *A&A*, 528, 151
- Kaper, L., Henrichs, H. F., Nichols, J. S., Snoek, L. C., Volten, H., Zwarthoed, G. A. A., 1996, *A&AS*, 116, 257
- Marcolino, W. L. F., Bouret, J.-C., Martins, F., Hillier, D. J., Lanz, T., Escolano, C., 2009, *A&A*, 498, 837
- Martins, F., Donati, J.-F., Marcolino, W. L. F., Bouret, J.-C., Wade, G. A., Escolano, C., Howarth, I. D., 2010, *MNRAS*, 407, 1423 (Paper I)
- Nazé, Y., Vreux, J., Rauw, G., 2001, *A&A*, 372, 195
- Nazé, Y., Rauw, G., Vreux, J., De Becker, M., 2004, *A&A*, 417, 667
- Nazé, Y., ud-Doula, A., Spano, M., Rauw, G., De Becker, M., Walborn, N. R., 2010, *A&A*, 520, 59
- Shore, S. N., Brown, D. N., Sonneborn, G., Landstreet, J. D., Bohlender, D. A., 1990, *ApJ*, 348, 242
- Simón-Díaz, S., Herrero, A., Uytterhoeven, K., Castro, N., Aerts, C., Puls, J., 2010, *ApJL*, 720, L174
- Smith, M. A., Fullerton, A. W., 2005, *PASP*, 117, 13
- Stahl, O., Kaufer, A., Rivinius, Th, et al., 1996, *A&A*, 312, 539
- ud-Doula, A., 2008, *Proceedings of the Workshop Clumping in Hot Star Winds*, Potsdam, 125
- ud-Doula, A., Owocki, S. P., 2002, *ApJ*, 576, 413
- ud-Doula, A., Owocki, S. P., Townsend, R. H. D., 2009, *MNRAS*, 392, 1022
- ud-Doula, A., Townsend, R. H. D., Owocki, S. P., 2006, *ApJL*, 640, L191
- Wade, G. A., et al., 2011, *MNRAS*, in press
- Wade, G. A., et al., 2011b, *MNRAS*, 416, 3160
- Walborn, N. R., 1972, *AJ*, 77, 312
- Walborn, N. R., Howarth, I. D., Herrero, A., Lennon, D. J., 2003, *ApJ*, 588, 1025
- Walborn, N. R., Sota, A., Maíz Apellániz, J., Alfaro, E. J., Morrell, N. I., Barbá, R. H., Arias, J. I., Gamen, R. C., 2010, *ApJL*, 711, L143